Available online at www.sciencedirect.com

ScienceDirect

Chinese Journal of Natural Medicines 2021, **19**(3): 212-224
doi: 10.1016/S1875-5364(21)60023-7

Chinese Journal of Natural Medicines

•Research article•

Comparative metabolism study on chlorogenic acid, cryptochlorogenic acid and neochlorogenic acid using UHPLC-Q-TOF MS coupled with network pharmacology

LI Jie[1, 2Δ], WANG Shao-Ping[1Δ], WANG Yu-Qi[2], SHI Lei[3], ZHANG Ze-Kun[2], DONG Fan[2], LI Hao-Ran[1], ZHANG Jia-Yu[1*], MAN Yu-Qing[3*]

[1] *School of Pharmacy, Binzhou Medical University, Yantai 264003, China;*
[2] *School of Chinese Pharmacy, Beijing University of Chinese Medicine, Beijing 102488, China;*
[3] *School of Pharmacy, Shandong University of Traditional Chinese Medicine, Jinan 250300, China;*
[4] *Department of Pharmacy, Binzhou Medical University Hospital, Binzhou 256603, China*

[ABSTRACT] Chlorogenic acid (5-CQA), neochlorogenic acid (3-CQA), and cryptochlorogenic acid (4-CQA), usually simultaneously exist in many traditional Chinese medicines (TCMs). However, insufficient attentions have been paid to the comparative metabolism study on these three isomeric constituents with similar effects on anti-inflammation until now. In this study, a novel strategy was established to perform comparative analysis of their metabolic fates in rats and elucidate the pharmacological mechanism of anti-inflammation. Firstly, diagnostic product ions (DPIs) deduced from the representative reference standards were adopted to rapidly screen and characterize the metabolites in rat plasma, urine and faeces using UHPLC-Q-TOF MS. Subsequently, Network pharmacology was utilized to elucidate their anti-inflammatory mechanism. Consequently, a total of 73 metabolites were detected and characterized, including 50, 47 and 43 metabolites for 5-CQA, 4-CQA and 3-CQA, orderly. Moreover, the network pharmacology study indicated that these three isomeric constituents and their major metabolites with similar *in vivo* metabolic pathways exerted anti-inflammatory effects through co-owned 20 biological processes, which involved 10 major signal pathways and 159 potential targets. Our study shed light on the similarities and differences of the metabolic profiling and anti-inflammatory activity among these three isomeric constituents and set an example for the further researches on the active mechanism of isomeric constituents existing in TCMs based on comparative metabolism study.

[KEY WORDS] Chlorogenic acid; Comparative metabolism study; Isomeric constituents; Anti-inflammation; UHPLC-Q-TOF MS; Network pharmacology

[CLC Number] R96, R917 **[Document code]** A **[Article ID]** 2095-6975(2021)03-0212-13

Introduction

A wide range of chemical constituents are the secondary metabolic products distributing in numerous plant species. Therefore, it is a common phenomenon that a great many isomeric constituents existing in traditional Chinese medicines (TCMs). Classically, these isomeric constituents with similar skeleton structures are much more likely to exhibit similar pharmacological activities and pharmacokinetic properties [1], even though some certain constituents may possess different or even opposite pharmacological effects [2-3].

Chlorogenic acid (5-caffeoyl qunic acid, 5-CQA), the most famous phenolic acids in TCMs and Chinese herbal products (*Lonicera japonica*, *Forsythia suspensa*, *Gardenia jasminoides*, *Shuanghuanglian* oral solution, *Yinhuang* granule, *etc*) and the most abundant polyphenol existing in human diet [4-5], has attracted wide publicity in past two decades. It is well known for the remarkable biological properties including heat-clearing [6-7], detoxifying [8], anti-inflammatory and antibacterial effects [9] *etc*. Meanwhile, 5-CQA is the most important member of chlorogenic acids (CGAs) family, which consists of quinic acid combining with one to four residues of certain cinnamic acids, most commonly caffeic

[Received on] 17-Jun.-2020
[Research funding] This work was supported by the Young and Creative Team for Talent Introduction of Shandong Province (No. 10073004), Binzhou Medical University Scientific Research Fund for High-level Talents (Nos. 2019KYQD06 and BY2018KYQD11), the Locality-University Cooperation Project of Yantai City (No. 2019XDRHXMPT18) and the Ability Establishment of Sustainable Use for Valuable Chinese Medicine Resources (No. 2060302).
[*]**Corresponding author]** Tel: 86-535-6913719, E-mail: zhangjiayu0615@163.com (ZHANG Jia-Yu); Tel: 86-543-3258550, E-mail: myq388@126.com (MAN Yu-Qing)
[Δ]These authors contributed equally to this work.
These authors have no conflict of interest to declare.

acid, *p*-coumaric acid and ferulic acid. Ordinarily, 5-CQA has several positional isomers, such as neochlorogenic acid (3-CQA), cryptochlorogenic acid (4-CQA) (Fig. S1), while 1-CQA was less commonly seen or low-contents bearing in TCMs. The structural differences of 3-CQA, 4-CQA and 5-CQA lie in the substitution sites of hydroxyl group replaced on quinic acid. Nowadays, most attentions have been paid to the metabolic fate of 5-CQA in various biosamples, while the comparative metabolism studies on 5-CQA, 4-CQA and 3-CQA have not been studied systematically yet, although the isomeric constituents theoretically might undergo similar biotransformation reactions *in vivo*. However, it is still unclear that their metabolic profiling is identical or not. Accordingly, the *in vivo* metabolism-correlated active mechanism of the co-owned anti-inflammatory pharmacological activity remains further studies.

With the development of analytical technologies, ultra-high performance liquid chromatography coupled with quadrupole time-of-flight mass spectrometry (UHPLC-Q-TOF MS) has shown excellent performance in the metabolite identification [10]. It usually serves as a rapid analysis platform for the complex chemical constituents owing to high chromatographic resolution, enhanced retention time reproducibility and improved sensitivity and selectivity. Herein, an UHPLC-Q-TOF MS based strategy was established to perform the comprehensive profiling and identification of drug metabolites in rat plasma, urine and faeces after the respective oral administration of 5-CQA, 4-CQA and 3-CQA to rats. The full scan-ddMS^2 data-acquisition method coupled with multiple data-mining techniques, including multiple mass defect filters (MMDFs) and diagnostic product ions (DPIs), was applied to improve the metabolite identification efficiency [11].

Moreover, network pharmacology is a novel, promising, cost-effective development approach based on bioinformatics systems biology and poly-pharmacology [12]. Instead of the traditional model "one drug, one target", Network Pharmacology provides a good understanding of the principles of networks and systems biology, and it has been considered to be the new pattern in drug discovery. Now, more and more unknown mechanisms of herbal medicines and their patent medicines are being gradually revealed by Network Pharmacology [13-14].

Although the anti-inflammatory mechanisms of 5-CQA and its two isomers had been studied many times, the anti-inflammatory activities of their metabolites *in vivo* were rarely concerned. Exactly, in this study, we first clarified the metabolic behavior of 5-CQA and its two isomers in normal Sprague Dawley (SD) rats with UHPLC-Q-TOF MS analysis platform. Secondly, the high-quality mass spectrometry data of CQAs metabolites including phase I and phase II metabolites were obtained. By comparing all the data, we finally obtain the key products, which might demonstrate different anti-inflammatory mechanisms compared with their prototype compounds. Therefore, the physiological activities of these metabolites were finally explored using Network Pharmacology, and a substantial relationship between the CQAs metabolites *in vivo* and their physiological activities was constructed.

Materials and Methods

Chemicals and materials

Reference standards including 5-CQA, 3-CQA, 4-CQA, caffeic acid, quinic acid, ferulic acid, isoferulic acid, were all purchased from Chengdu Biopurify Phytochemicals Co., Ltd. (Chengdu, China). Their structures were fully elucidated by comparison of their spectral data (ESI-MS and ^{1}H, ^{13}C NMR) with those published literature values. Their purities were all determined to be higher than 98% by HPLC-UV analysis.

HPLC grade acetonitrile, methanol and formic acid (FA) were purchased from Thermo Fisher Scientific (Fair Lawn, NJ, USA). Ultrapure water used in the experiment was prepared by a Milli-Q system (Millipore, MA, USA). All the other chemicals of analytical grade were available at the workstation, Beijing Chemical Works (Beijing, China). Grace Pure™ SPE C_{18}-low solid-phase extraction cartridges (200 mg/3 mL, 59 μm, 70 Å) for the pretreatment of biological samples were supplied by Grace Davison Discovery Science™ (Deerfield, IL, USA).

Animals

Male SD rats weighing 220 ± 10 g [certification number SCXK (Jing 2016-0006)] were provided by Beijing Vital River Laboratory Animal Technology Co. (Beijing, China). Twelve SD rats were raised in SPF level conditions in Beijing University of Chinese Medicine with stable temperature of 22−24 °C and humidity of 55%−65%. All the SD rats were allowed free access to water and food during one week's acclimation with 12 h light/dark cycle. After for, they were randomly divided into four groups including Control group, 5-CQA group, 4-CQA group and 3-CQA group. They were fasted 12 h prior to the experiment with free access to water.

Drug administration and biological samples preparation

The standards were suspended in normal saline. Then rats in different drug groups were orally given at a dose of 250 mg/kg body weight. Normal saline solution (2 mL) was administrated to rats in Control Group. Blood samples (0.8 mL) were taken from the suborbital venous plexus of rats at 0.5, 1.0, 1.5, 2 and 4 h post-administration. Samples of urine and faeces were respectively collected 0−24 h after the oral administration. Each faeces sample (2.0 g) was dissolved in deionized water with an ultrasonic processing for 60 min. Finally, all the biosamples were centrifuged at 3000 $r \cdot min^{-1}$ for 15 min to obtain supernatant, and then the samples in the same group were merged into one collective sample. All these samples were stored at −80 °C prior to the LC-MS analysis.

The concentration and purification of all biological samples were prepared by Grace Pure™ SPE columns. Plasma, urine and faeces samples (1.0 mL) were respectively loaded into the SPE cartridges, which were successively pretreated with 5 mL methanol and 5 mL deionized water. And

then, the SPE cartridges were washed with deionized water (5.0 mL) and methanol (3.0 mL) in proper order. The methanol eluate was collected and dried under high purity nitrogen at room temperature. The residue was re-dissolved in 100 μL of acetonitrile/water (2 ∶ 98, *V*/*V*) and then centrifuged at 14 000 r·min^{-1} for 15 min. The supernatant (3.0 μL) was injected into the LC-MS instrument for analysis.

Instrument and conditions

The UHPLC analyses were performed using an Exion-LC™ AC liquid chromatography system (Shimadzu, Japan) with a binary pump and an autosampler. Q-TOF mass spectrometer coupled with dual-spray TurboV ion source (X500R Q-TOF, AB SCIEX, Foster City, CA, USA) equipped with a high electrospray ionization (HESI) source. The chromatographic separation was carried out at 40 °C using a Waters HSS T3 UPLC column (2.1 mm × 100 mm, 1.7 μm; Waters Corporation, Milford, MA, USA). The mobile phase consisted of 0.1% (*V*/*V*) formic acid (A)–acetonitrile (B) at a flow rate of 0.30 mL·min^{-1} and the linear gradient procedure was described as follows: 0–6 min, 2%–10% B; 6–10 min, 10%–25% B; 10–15 min, 25%–35% B; 15–16 min, 35%–40% B; 16–20 min, 40%–80% B; 20–21 min, 80%–95% B; 21–24 min, 95% B.

Analyses on an UHPLC-Q-TOF were performed using simultaneous MS^1 and MS/MS (IDA) acquisition. The parameters were set as follows: HESI polarity, negative; curtain gas, 35; ion source gas 1, 60 psi; ion source gas 2, 60 psi; temperature, 550 °C; ion spray voltage floating, 4.5 kV; declustering potential, 80 V; MS^1 accumulation time, 100 ms; MS^1 mass range, *m*/*z* 100–1000; MS/MS accumulation time, 10 ms; cycle time, 640 ms; Q1 window, 20 Da; collision energy, 45 eV; collision energy spread, 15 eV. The mass calibration was automatically performed every 5 injections using a HESI negative calibration solution *via* an inbuilt CDS. Online MDF windows were set to ± 50 mDa.

Peak selections and data processing

Acquisition and processing of all the data were carried out by SCIEX OS 1.3 workstation from AB SCIEX. To obtain as many fragment ions as possible, chromatographic peaks with intensities over 30 000 were selected for identification. All the relevant data, including peak number, retention time, accurate mass, predicted chemical formula, and corresponding mass error, were summarized in Table 1. The chemical formulas for all the parent ions were calculated from the accurate mass using a formula predictor by setting the parameters as follows: C [0–30], H [0–50], O [0–30], S [0–3], N [0–3] and ring double bond (RDB) equivalent value [0–15]. Other elements, such as P and Br, were not considered as they rarely presented in the complex matrix. Potential metabolites discovery involved parameters were set as follows: Firstly, biotransformation covers extensive phase I and phase II metabolism. Then minimum peak width was set to 5.0 sec, and the minimum chromatographic intensity was set to 500 cps. The maximum mass errors between the measured and calculated values were fixed within 10 ppm.

Mechanism study on anti-inflammation about metabolites based on network pharmacology

The prediction of putative targets of inflammation and compounds

Putative genes related to inflammation were obtained

Table 1 The identified metabolites *in vivo* of 3-CQA, 5-CQA and 4-CQA in rats

Peak	t_R/ min	Formula [M – H]	Theoretical Mass (*m*/*z*)	Experimental Mass (*m*/*z*)	Error (ppm)	ESI-MS/ MS fragment ions	Identification/ Reactions	5-CQA	4-CQA	3-CQA
M1	0.88	$C_9H_9O_5$	197.044 45	197.045 80	6.9	MS^2 [197]: 149 (100)*, 121 (80), 167 (23)	Syringic acid	√	√	√
M2	0.93	$C_7H_{11}O_6$	191.055 01	191.056 14	5.9	MS^2 [191]: 173 (100)*, 155 (63), 111 (43), 127 (15)	Quinic acid *	√	√	√
M3	3.67	$C_7H_9O_5$	173.044 45	173.045 72	7.3	MS^2 [173]: 129 (100), 155 (36), 111 (23)	Shikimic acid		√	√
M4	4.78	$C_9H_7O_2$	147.045 40	147.045 43	0.2	MS2 [147]: 103 (100)	Cinnamic acid	√	√	√
M5	5.33	$C_8H_7O_4$	167.033 88	167.034 97	6.5	MS^2 [167]: 167 (100), 124 (47), 140 (13)	Vanillic acid	√	√	√
M6	5.42	$C_{16}H_{20}O_{12}S$	435.059 17	435.060 93	4.0	MS^2 [435]: 261 (100), 417 (70), 181 (38), 163 (43)	Sulfonation, hydrogenation	√		
M7	5.77	$C_8H_7O_4$	167.033 88	167.035 40	9.1	MS^2 [167]: 123 (100), 149 (22)*, 137 (18)	Vanillic acid	√		
M8	5.89	$C_8H_7O_4$	167.033 88	167.035 50	9.7	MS^2 [167]: 123 (100), 167 (56)	Vanillic acid	√		
M9	6.14	$C_{11}H_{10}NO_5$	236.055 34	236.057 07	7.3	MS^2 [236]: 162 (100), 134 (34)*	Caffeic acid-glycine	√	√	√
M10	6.15	$C_9H_9O_5$	197.044 45	197.046 01	7.9	MS^2 [197]: 123 (100), 135 (34)*	Syringic acid			√
M11	6.24	$C_7H_5O_4$	153.018 23	153.019 64	9.2	MS^2 [153]: 109 (100)	3, 4-dihydroxybenzoic acid	√		
M12	6.31	$C_9H_9O_7S$	261.006 35	261.007 54	4.6	MS^2 [261]: 181 (100), 135 (33)*	Dihydrocaffeic acid sulfated conjugate	√	√	√
M13	6.49	$C_8H_7O_4$	167.033 88	167.035 42	9.2	MS^2 [167]: 123 (100), 167 (43), 149 (9)*	Vanillic acid		√	

Continued

Peak	t_R/ min	Formula [M – H]	Theoretical Mass (*m/z*)	Experimental Mass (*m/z*)	Error (ppm)	ESI-MS/ MS fragment ions	Identification/ Reactions	5-CQA	4-CQA	3-CQA
M14	6.57	$C_9H_8NO_3$	178.049 86	178.051 14	7.2	MS^2 [178]: 178 (100)*, 150 (78), 160 (68)	Hippuric acid	√		
M15	6.83	$C_{16}H_{17}O_{12}S$	433.043 52	433.045 25	4.0	MS^2 [433]: 433 (100), 415 (79), 389 (78), 153 (42), 191 (17)*	Sulfonation	√		
M16	6.89	$C_9H_9O_4$	181.049 53	181.050 58	5.8	MS^2 [181]: 137 (100)	Dihydrocaffeic acid		√	√
M17	6.91	$C_{16}H_{19}O_9$	355.102 35	355.103 88	4.3	MS^2 [355]: 181 (100), 137 (30), 173 (16)*, 191 (11), 267 (9)	Hydrogenation		√	
M18	6.93	$C_{16}H_{17}O_9$	353.086 71	353.086 82	0.3	MS^2 [353]: 191 (100)*, 179 (63)*, 135 (58)*	3-CQA *	√	√	√
M19	7.00	$C_9H_9O_7S$	261.006 35	261.007 99	6.3	MS^2 [261]: 137 (100), 181 (12)	Dihydrocaffeic acid sulfated conjugate	√		√
M20	7.24	$C_9H_9O_4$	181.049 53	181.050 76	6.8	MS2 [181]: 137 (100)	Dihydrocaffeic acid	√		
M21	7.26	$C_{16}H_{17}O_9$	353.086 71	353.087 60	2.5	MS^2 [353]: 191 (100)*, 179 (75)*, 135 (46)*	5-CQA isomer	√		
M22	7.43	$C_7H_5O_3$	137.023 32	137.024 59	9.3	MS^2 [137]: 137 (100), 93 (54), 136 (31), 109 (11)	3-hydroxybenzoic acid	√	√	√
M23	7.77	$C_9H_8NO_4$	194.044 78	194.046 40	8.3	MS^2 [194]: 135 (100*), 150 (72)	3-hydroxyl hippuric acid	√	√	√
M24	7.93	$C_{16}H_{17}O_{12}S$	433.043 52	433.044 90	3.2	MS^2 [433]: 433 (100), 153 (60), 397 (50), 173 (34)*, 191 (22)*, 353 (21)	Sulfonation	√		
M25	8.05	$C_{11}H_9O_5$	221.044 44	221.045 86	6.4	MS^2 [221]: 159 (100)	Caffeic acid-acetylation	√		
M26	8.10	$C_{23}H_{29}O_{14}$	529.119 90	529.120 53	1.2	MS^2 [529]: 191 (100)*, 337 (63), 161 (38), 353 (18), 193 (12)	Glucuronidation	√		
M27	8.13	$C_9H_9O_7S$	261.006 35	261.007 47	4.3	MS^2 [261]: 181 (100), 137 (38), 167 (35)	Dihydrocaffeic acid sulfated conjugate	√		√
M28	8.25	$C_{16}H_{17}O_9$	353.086 71	353.088 59	5.3	MS^2 [353]: 179 (100)*, 173 (90*), 191 (74)*, 135 (62)*	5-CQA isomer	√	√	
M29	8.26	$C_9H_7O_7S$	258.991 80	258.992 64	3.2	MS^2 [259]: 153 (100), 125 (76), 135 (41)*, 179 (36)*	Sulfate conjugate of caffeic acid		√	
M30	8.32	$C_9H_9O_7S$	261.006 35	261.007 86	5.8	MS^2 [261]: 181 (100), 137 (38), 179 (8)*	Dihydrocaffeic acid sulfated conjugate	√		√
M31	8.54	$C_{23}H_{29}O_{14}$	529.119 90	529.120 85	1.8	MS^2 [529]: 179 (100)*, 173 (74)*, 191 (55)*, 353 (55), 337 (18), 135 (13)*	Glucuronidation	√		
M32	8.56	$C_9H_9O_4$	181.049 53	181.050 75	6.7	MS^2 [181]: 137 (100)*	Dihydrocaffeic acid	√	√	√
M33	8.59	$C_{16}H_{17}O_9$	353.086 71	353.087 99	3.6	MS^2 [353]: 191(100)*, 135(68)*	5-CQA isomer		√	√
M34	8.61	$C_9H_8NO_3$	178.049 86	178.051 07	6.8	MS^2 [178]: 134 (100), 150 (90)	Hippuric acid	√	√	√
M35	8.64	$C_{10}H_9O_4$	193.049 53	193.050 76	6.4	MS^2 [193]: 149 (100)*	Ferulic acid isomer			√
M36	8.84	$C_{16}H_{17}O_9$	353.086 71	353.087 17	1.3	MS^2 [353]: 191 (100)*, 179 (68)*, 135 (60)*, 173 (56)*	5-CQA *	√	√	√
M37	8.89	$C_9H_7O_4$	179.033 88	179.035 33	8.1	MS^2 [179]: 135 (100)*, 134 (50)*, 91 (50)	Caffeic acid isomer	√	√	
M38	8.92	$C_{17}H_{19}O_9$	367.102 36	367.103 74	3.8	MS^2 [367]: 193 (100)*, 134 (92)*, 191 (34)*	Methylation	√	√	√
M39	9.01	$C_9H_9O_4$	165.054 60	165.055 88	7.8	MS^2 [165]: 121 (100), 135 (72)*	3-hydroxyphenylpropionic acid	√		√
M40	9.08	$C_{10}H_9O_7S$	273.007 40	273.007 60	0.7	MS^2 [273]: 193 (100), 134 (51)*, 178 (43)*, 149 (22)*	Sulfate conjugate of methyl caffeic acid	√	√	√
M41	9.08	$C_{17}H_{21}O_9$	369.118 01	369.120 44	6.6	MS^2 [369]: 195 (100), 173 (8)*	Methylation, hydrogenation	√	√	√
M42	9.17	$C_9H_7O_4$	179.033 88	179.035 26	7.7	MS^2 [179]: 135 (100)*, 161 (56)*, 134 (25)*, 107 (10)	Caffeic acid *	√	√	√
M43	9.22	$C_{10}H_{11}O_4$	195.065 18	195.066 67	7.6	MS^2 [195]: 150 (100), 122 (31), 165 (30), 180 (10), 108 (7)	Dihydro-ferulic acid		√	

Continued

Peak	t_R/ min	Formula [M – H]	Theoretical Mass (*m/z*)	Experimental Mass (*m/z*)	Error (ppm)	ESI-MS/ MS fragment ions	Identification/ Reactions	5-CQA	4-CQA	3-CQA
M44	9.23	$C_{10}H_{11}O_3$	179.070 27	179.071 59	7.4	MS^2 [179]: 135 (100)*, 91 (98), 178 (60)*	Methyl 2-ethoxybenzoate		√	√
M45	9.24	$C_7H_5O_2$	121.028 40	121.028 85	3.7	MS^2 [121]: 121 (100), 93 (25)	Benzoic acid	√	√	√
M46	9.28	$C_{23}H_{29}O_{14}$	529.119 90	529.121 67	3.3	MS^2 [529]: 191 (100)*, 337 (39), 353 (31), 161 (22), 179 (14)*	Glucuronidation	√		
M47	9.31	$C_{16}H_{19}O_9$	355.102 35	355.103 94	4.5	MS^2 [355]: 173 (100), 160 (82), 191 (26)	Hydrogenation		√	
M48	9.38	$C_9H_7O_3$	163.038 97	163.040 30	8.2	MS2 [163]: 101 (8), 119 (7)	Coumaric acid		√	√
M49	9.39	$C_{17}H_{19}O_9$	367.102 36	367.103 14	2.1	MS^2 [367]: 193 (100), 134 (78)*, 178 (5)*	Methylation	√	√	√
M50	9.41	$C_{10}H_9O_4$	193.049 53	193.050 94	7.3	MS^2 [193]: 134 (100)*	Isoferulic acid *	√		√
M51	9.47	$C_{16}H_{17}O_9$	353.086 71	353.086 93	0.6	MS^2 [353]: 191 (100)*	4-CQA *	√		
M52	9.51	$C_{17}H_{21}O_9$	369.118 01	369.119 55	4.2	MS^2 [369]: 191 (100)*, 173 (23)*, 137 (6)	Methylation, Hydrogenation		√	√
M53	9.52	$C_9H_7O_4$	179.033 88	179.035 22	7.5	MS^2 [179]: 135 (100)*	Caffeic acid isomer		√	
M54	9.73	$C_9H_9O_4$	181.049 53	181.050 93	7.7	MS^2 [181]: 137 (100), 163 (25)	Dihydrocaffeic acid		√	
M55	9.83	$C_{17}H_{21}O_9$	369.118 01	369.119 56	4.2	MS^2 [369]: 173 (100)*	Methylation, Hydrogenation		√	√
M56	9.85	$C_{10}H_{11}O_4$	195.065 18	195.066 54	7.0	MS^2 [195]: 180 (100), 163 (45), 134 (20)*	Dihydro-ferulic acid		√	
M57	10.02	$C_{17}H_{21}O_9$	369.118 01	369.119 76	4.7	MS^2 [369]: 369 (100), 173 (73)*, 191 (65)*	Methylation, Hydrogenation	√	√	√
M58	10.10	$C_{17}H_{19}O_9$	367.102 36	367.102 25	−0.3	MS^2 [367]: 173 (100)*, 191 (43)*, 134 (32)*, 193 (18)	Methylation	√	√	√
M59	10.23	$C_{17}H_{21}O_9$	369.118 01	369.120 11	5.7	MS^2 [369]: 191 (100)*, 173 (21)*, 181 (17), 137 (6)	Methylation, Hydrogenation		√	
M60	10.24	$C_8H_7O_2$	135.044 06	135.045 40	9.9	MS^2 [135]: 135 (100)*, 120 (83), 92 (45)	Vinylcatechol	√	√	√
M61	10.32	$C_{17}H_{21}O_9$	369.118 01	369.119 15	3.1	MS^2 [369]: 369 (100), 173 (98)*, 191 (68)*	Methylation, Hydrogenation		√	√
M62	10.42	$C_9H_9O_5$	197.044 45	197.045 80	6.9	MS^2 [197]: 153 (100), 182 (96), 123 (84), 137 (45)	Syringic acid	√	√	
M63	10.42	$C_{17}H_{19}O_9$	367.102 36	367.102 86	1.4	MS^2 [367]: 173 (100)*, 193 (25), 134 (24)*	Methylation	√	√	√
M64	10.67	$C_{10}H_{11}O_4$	195.065 18	195.066 65	7.5	MS^2 [195]: 121 (100), 136 (40)	Dihydro-ferulic acid	√		
M65	10.72	$C_9H_9O_4$	165.054 60	165.055 85	7.6	MS^2 [165]: 121 (100), 135 (72)*	3-hydroxyphenylpropionic acid	√		√
M66	10.79	$C_9H_9O_4$	179.033 88	179.035 22	7.5	MS^2 [179]: 135 (100)*, 134 (70)*, 107 (14)	Caffeic acid isomer			√
M67	11.04	$C_{16}H_{19}O_9$	355.102 36	355.099 23	−8.8	MS^2 [355]: 167 (100), 181 (85), 137 (56), 275 (23)	Hydrogenation		√	√
M68	11.05	$C_{10}H_9O_4$	193.049 53	193.050 85	6.8	MS^2 [193]: 134 (100)*, 178 (35)*, 149 (13)*, 106 (7)	Ferulic acid *			√
M69	11.42	$C_{10}H_{11}O_4$	195.065 18	195.066 23	5.4	MS^2 [195]: 180 (100), 152 (9)	Dihydro-ferulic acid	√	√	
M70	12.69	$C_{10}H_9O_4$	193.049 53	193.050 96	7.4	MS^2 [193]: 134 (100)*, 149 (56)*	Ferulic acid isomer	√		
M71	13.53	$C_{10}H_9O_4$	193.049 53	193.051 35	9.4	MS^2 [193]: 134 (100)*, 149 (46)*	Ferulic acid isomer		√	
M72	13.82	$C_{24}H_{31}O_{14}$	543.170 83	543.171 72	1.6	MS^2 [543]: 367 (100), 349 (34), 173 (12)*, 129 (13)	Methylation, Glucuronidation of CQA	√	√	√
M73	14.15	$C_{15}H_{17}O_{10}$	357.081 62	357.078 55	−8.6	MS^2 [357]: 357 (100), 313 (48), 163 (28)	Hydrolysis, Glucuronidation of Dihydrocaffeic acid	√	√	√

t_R: retention time; √: detected; *: DPIs

from National Center for Biotechnology Information (NCBI) Gene Database (https://www.ncbi.nlm.nih.gov/), UniProt database (https://www.uniprot.org/) and Online Mendelian Inheritance in Man database (http://www.omim.org/) using "inflammation" as a keyword and species just set as "Homo sapiens" [15-16]. Potential targets of the aimed compounds were obtained from Traditional Chinese Medicine Systems Pharmacology Database Analysis Platform (http://tcmspw.com/tcmsp.php) and PubChem database (https://pubchem.ncbi.nlm.nih.gov/). Based on the above results, the common targets were obtained through comparative analysis by Bioinformatics & Evolutionary Genomics Database (http://bioinformatics.psb.ugent.be/webtools/Venn/) of potential inflammation targets and compound targets.

Network construction and its characteristics

To facilitate scientific interpretation of the complex relationships between compounds and related predictive targets, Network of compound-related target was established using Cytoscape software (version 3.7.2, USA). At the same time, the possible information on inter-protein interactions was mined by importing common targets of potential inflammation targets and compound targets to the STRING database (https://string-db.org/cgi/input) [17], which play a role of a station for all information on functional links between targets. To ensure the accuracy of the results, only "Homo sapiens" targets with *P*-vaule score higher than 0.01 were picked out. Three topological network features including "degree", "betweenness" and "closeness" were calculated. The close relationship between attributes in different networks was represented by "nodes". When the number on connected edges of a node was more than 2 times that of other nodes, it would be considered as a key node [17].

Pathway enrichment and gene ontology analysis

Pathway enrichment and gene ontology analysis were presented on the proteins involved in the protein-protein interaction (PPI) network using Kyoto Encyclopedia of Genes and Genomes (KEGG, https://www.kegg.jp/) database and DAVID database (https://david.ncifcrf.gov/). Relevant pathways and GO terms with *P*-value less than 0.01 were selected as the significant signaling pathways [18-19].

Results

A summarized diagram of presently developed analytical strategy and methodology for the comparative study of CQA isomers based on metabolite identification *in vivo* and Network Pharmacology was illustrated in Fig. 1.

Analytical strategy for metabolite identification

In order to accomplish the systematic screening and characterization of metabolites, an analytical strategy was developed on the UHPLC-high resolution MS instrument with multiple data acquisition and processing techniques. Firstly, the full scan ESI-MS and ESI-MS/MS data sets of all the biosamples were acquired based on data-dependent acquisition method. Then, considering the metabolites generated from the prototype drug usually possess similar skeleton structure, they could be screened by MDF filtering (MS^1 level), which could be applied to trace the primary metabolites, especially the unknown drug metabolites. Therefore, several MDF templates were used in parallel based on the structures of 5-CQA, 3-CQA and 4-CQA: (1) parent drug (*m*/*z* 353.0867), the core nucleus such as caffeic acid (*m*/*z* 179.0339) and quinic acid (*m*/*z* 191.0550); (2) the GSH conjugation (*m*/*z* 660.1715), glycosylation (*m*/*z* 515.1404), glucuronide conjugation (*m*/*z* 529.1199), and sulfate conjugation (*m*/*z* 433.0435) of CQA. Specifically, each MDF window was set to ±50 mDa around the mass defects of the templates over a mass ranging of ±50 Da around the filter template masses.

For the subsequent data-mining processing, SCIEX OS 1.3 workstation was adopted to filter the known and unknown metabolites. The high-resolution extracted ion chromatogram (HREIC) process with *m*/*z* values calculated is highly effective in discovering the known metabolites. Meanwhile, Metabolite Pilot™ software was used to analyze the unknown metabolites, and thus the metabolite candidates were screened out. Finally, a combination of data mining methods including neutral loss fragments (NLFs) and diagnostic product ions (DPIs, shown in Fig. 2) were performed to rapidly identify and confirm the multiple metabolites according to the ESI-MS/MS level searching. In addition, the ESI-MS/MS spectra of reference standards were illustrated in Fig. S2.

Characterization of 5-CQA, 4-CQA and 3-CQA metabolites in rats

As a result, a total of 73 metabolites were detected and characterized in rat urine, plasma and faeces samples attributed to 5-CQA group, 4-CQA group and 3-CQA group (50, 47 and 43, respectively) based on UHPLC-Q-TOF-MS/MS analysis coupled with the established analytical strategy. The detailed mass data of these detected metabolites were listed in Table 1, and the metabolite distribution in urine, plasma and faeces was summarized in Table S1.

M18, **M21**, **M28**, **M33**, **M36** and **M51** showed the same $[M-H]^-$ ions at *m*/*z* 353.086 71 ($C_{16}H_{17}O_9$, error ≤ ±10.00 ppm). They also presented the similar fragmentation patterns and produced the same DPIs compared with CQA standards, such as *m*/*z* 179.0350 (caffeic acid skeleton) through the neutral loss of *m*/*z* 174 ($C_7H_{10}O_5$). Furthermore, they all possessed characteristic secondary generation product ions at *m*/*z* 161.0224 and *m*/*z* 135.0452, which were formed by neutral loss of 18 Da (H_2O) and 44 Da (CO_2) individually from the ion at *m*/*z* 179.0350. The DPIs at *m*/*z* 191.0561 (quinic acid skeleton) and *m*/*z* 173.0455 ($[\text{quinic acid}-H_2O]^-$) were also observed. Finally, **M18**, **M36**, and **M51** were positively identified as the prototype drugs (3-CQA, 5-CQA and 4-CQA) based on the comparison of ESI-MS/MS spectra and retention times with the corresponding reference standards, respectively.

M37, **M42**, **M53** and **M66** were eluted at 9.17 min, 8.89 min, 10.79 min and 9.52 min, orderly. They afforded the deprotonated molecule ions at *m*/*z* 179.035 26 ($C_9H_7O_4$, mass

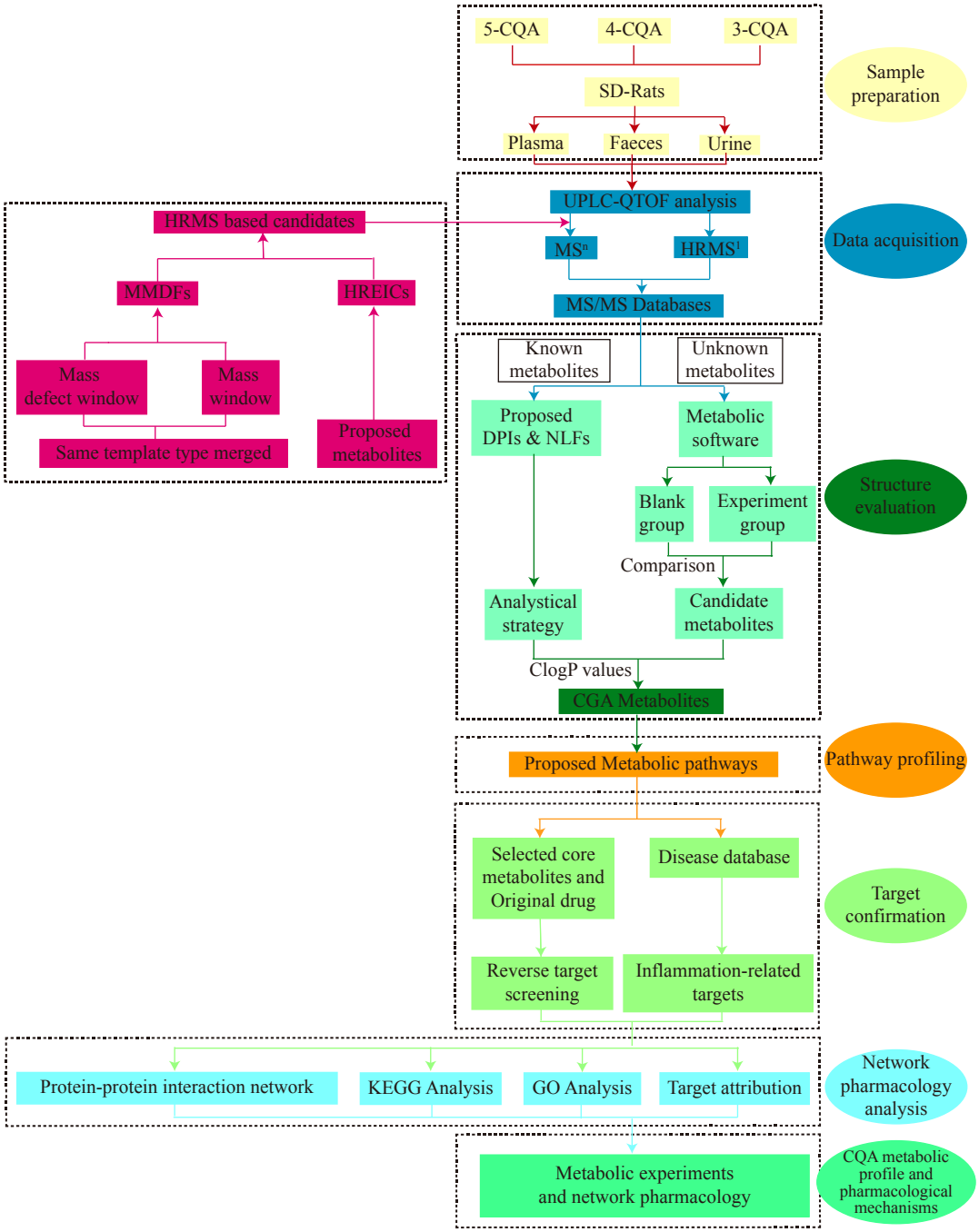

Fig. 1 Summary diagram of the developed strategy and methodology

error within ±10.00 ppm). Moreover, the DPI at *m/z* 135 $[M-H-CO_2]^-$ was observed in all of their ESI-MS^2 spectra, which suggested the presence of carboxyl group in their molecules. And thus, **M42** was positively identified as caffeic acid based on the comparison of ESI-MS/MS spectra and retention time with the corresponding reference standard, while the others were characterized as caffeic acid isomers [20].

M16, **M20**, **M32** and **M54** showed the same theoretical $[M-H]^-$ ions at *m/z* 181.049 53, which was calculated as $C_9H_9O_4$ based on the accurate mass with mass errors within ±10 ppm. In their ESI-MS^2 spectra, the intensively characteristic product ion at *m/z* 163 $[M-H-H_2O]^-$ was generated due to the neutral loss of H_2O (18 Da). In combination with the fragment ion at *m/z* 137 $[M-H-CO_2]^-$, they were finally identified as hydrogenation products of caffeic acid [21].

M25 showed the theoretical $[M-H]^-$ ion at *m/z* 221.044 44 ($C_{11}H_9O_5$, mass error of 6.4 ppm). It yielded the fragment ion at *m/z* 159, which indicated the existence of hydroxyl, methyl and carbon oxide group. Considering that it was 42 Da more than that of caffeic acid, **M25** was finally characterized as acetylation conjugation of caffeic acid [21].

M9 afforded $[M-H]^-$ ion at *m/z* 236.055 34 in the full-

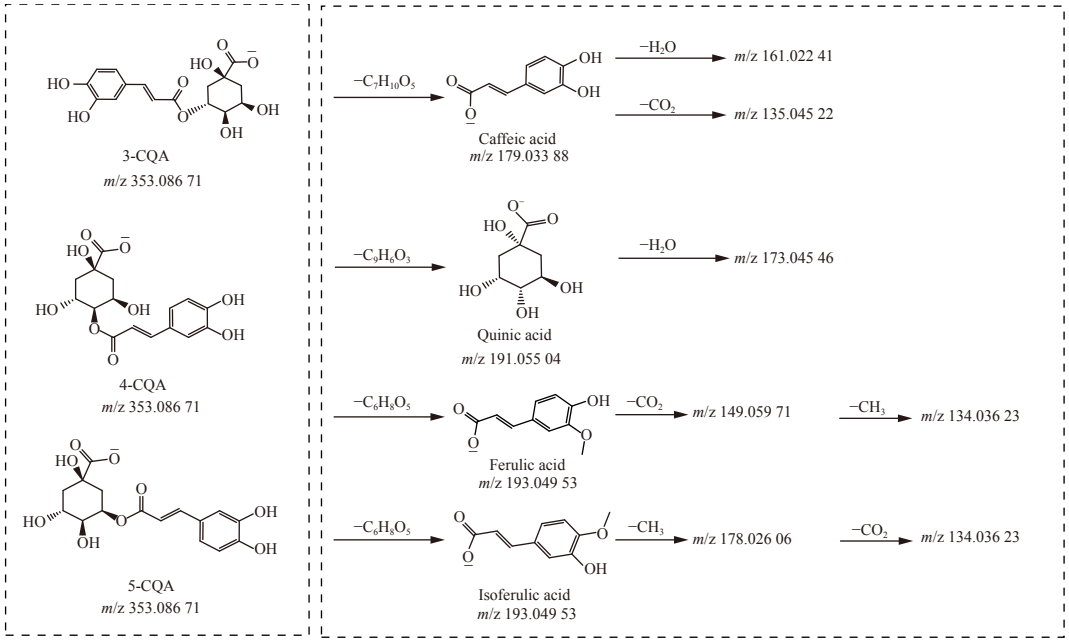

Fig. 2 The proposed DPIs for the representative reference standards

scan ESI-MS spectrum. It further yielded a series of product ions at *m/z* 162 ($[M - H - NH_2CH_2COO]^-$) and *m/z* 134 ($[M - H - C_2H_4NO_2 - CO]^-$) by loss of $C_2H_4NO_2$ and $C_3H_4NO_3$, respectively. And thus, **M9** was characterized as glycine conjugation of caffeic acid [21].

M73 eluted at 10.14 min afforded the deprotonated molecule ion at *m/z* 357.081 62 ($C_{15}H_{17}O_{10}$, mass error of −3.07 ppm). Furthermore, the ion at *m/z* 357 generated the product ions at *m/z* 313 $[M - H - CO_2]^-$ and *m/z* 163 $[M - H -$ glucuronide $- H_2O]^-$. Therefore, **M73** was characterized as glucuronide conjugation of dihydro-caffeic acid [21].

M4 displayed the theoretical $[M - H]^-$ ion at *m/z* 147.0454 ($C_9H_7O_2$, mass error within ±10.00 ppm). In the ESI-MS^2 spectrum, it yielded the product ion at *m/z* 103 $[M - H - CO_2]^-$. Considering that it was 32 Da less than that of caffeic acid, **M4** was tentatively characterized as cinnamic acid [22].

M48 afforded $[M - H]^-$ ion at *m/z* 163.038 97. Its formula could be interpreted as $C_9H_7O_3$ with mass error within ±2.00 ppm. It was 16 Da less than that of caffeic acid, indicating that **M48** might the dehydroxylation product of caffeic acid. Moreover, the product ions at *m/z* 119 $[M - H - CO_2]^-$ and *m/z* 101 $[M - H - CO_2 - H_2O]^-$ were also detected, suggesting the presence of carboxyl group and hydroxyl group in its molecule. Therefore, **M48** was tentatively characterized as coumaric acid [22].

M29 afforded the deprotonated molecule ion at *m/z* 258.991 80 ($C_9H_7O_7S$, mass error within ±10.00 ppm). It was 80 Da more than that of caffeic acid, which indicated that the sulfation reaction probably occurred during the biotransformation. Moreover, DPIs at *m/z* 179 $[M - H - SO_3]^-$ and *m/z* 135 $[M - H - SO_3 - CO_2]^-$ were also observed. Based on the above deduction and relevant biotransformation, **M29** was tentatively characterized as sulfate conjugate of caffeic acid [23].

With the retention times ranging from 6.31 to 8.32 min, **M12**, **M19**, **M27** and **M30** showed the same theoretical $[M - H]^-$ ions at *m/z* 261.006 35 ($C_9H_9O_7S$, mass error within ±10.00 ppm). In addition, DPIs at *m/z* 181 $[M - H - SO_3]^-$ and *m/z* 137 $[M - H - SO_3 - CO_2]^-$ appeared in their ESI-MS^2 spectra owing to the neutral loss of SO_3 and ($SO_3 + CO_2$), respectively. Therefore, they were all tentatively characterized as hydrogenation and subsequently sulfate conjugation of caffeic acid.

M40 eluted at 9.08 min gave $[M - H]^-$ ion at *m/z* 273.0074 ($C_{10}H_9O_7S$, mass error within ±10.00 ppm). It further yielded a series of characteristic product ions at *m/z* 178 ($[M - H - SO_3 - CH_3]^-$), *m/z* 149 ($[M - H - SO_3 - CO_2]^-$), *m/z* 134 ($[M - H - SO_3 - CO_2 - CH_3]^-$) and *m/z* 193 ($[M - H - SO_3]^-$). And thus, **M40** was tentatively characterized as methylation and sulfation conjugation of caffeic acid [24].

M35, **M50**, **M68**, **M70** and **M71** yielded $[M - H]^-$ ions at *m/z* 193.049 53 ($C_{10}H_9O_4$, mass error within ± 10.00 ppm). In the ESI-MS^2 spectra, the characteristic product ions at *m/z* 178 $[M - H - CH_3]^-$, *m/z* 149 $[M - H - CO_2]^-$ and *m/z* 134 $[M - H - CO_2 - CH_3]^-$ indicated the possible presence of carboxyl group and methyl group in their molecules. Among them, **M68** and **M50** could be positively identified as ferulic acid and isoferulic acid based on the comparison of ESI-MS/MS spectra and retention time with those of reference standards. And thus, the other three metabolites were characterized as ferulic acid isomers [24].

M60 afforded $[M - H]^-$ ion at *m/z* 135.044 06 ($C_8H_7O_2$, mass error within ±10.00 ppm) with the retention time of 10.24 min. Moreover, the ion at *m/z* 135 yielded the product ions at *m/z* 120 $[M - H - CH_3]^-$ and *m/z* 92 $[M - H - CO - CH_3]^-$, which suggested the presence of methyl group and

carbonyl group, respectively. According to the previous literature data, **M60** was tentatively characterized as vinylcatechol [25].

M39 and **M65** provided their deprotonated molecular ions at *m/z* 165.055 89 and *m/z* 165.055 84 ($C_9H_9O_4$, mass error within ±10.00 ppm), respectively. The product ion at *m/z* 121 $[M - H - CO_2]^-$ appeared in their ESI-MS^2 spectra, suggesting the presence of carbonyl group. Accordingly, both **M39** and **M65** were tentatively characterized as 3-hydroxyphenylpropionic acid or its isomer.

M43, **M56**, **M64** and **M69** showed the same $[M - H]^-$ ions at *m/z* 195.065 18 ($C_{10}H_{11}O_4$, mass error ≤ ±10.00 ppm), which presented the similar fragmentation patterns, DPIs and characteristic product ions. Besides, they were 2 Da more than that of ferulic acid, indicating that they were hydrogenation products of ferulic acid. The characteristic product ions at *m/z* 180 $[M - H - CH_3]^-$ and *m/z* 136 $[M - H - CH_3 - CO_2]^-$ appearing in their ESI-MS^2 spectra also confirmed our deduction. And thus, **M43**, **M56**, **M64** and **M69** were tentatively characterized as dihydro-ferulic acid and its isomers [26].

M2 afforded $[M - H]^-$ ion at *m/z* 191.056 14 ($C_7H_{11}O_6$, mass error ≤ ±10.00 ppm), and then yielded a series of DPIs at *m/z* 173 $[M - H - H_2O]^-$, *m/z* 147 $[M - H - CO_2]^-$ and *m/z* 111 $[M - H - CO_2 - 2H_2O]^-$. Based on the comparison of ESI-MS/MS spectrum and retention time with the corresponding reference standard, **M2** was unambiguously identified as quinic acid [21].

M3 afforded $[M - H]^-$ ion at *m/z* 173.044 45 ($C_7H_9O_5$, mass error ≤ ±10.00 ppm). which was 18 Da less than that of quinic acid, indicating that **M3** was likely to be dihydroxylation product of quinic acid. Meanwhile, the occurrence of product ions at *m/z* 129 $[M - H - CO_2]^-$, *m/z* 155 $[M - H - H_2O]^-$ and *m/z* 111 $[M - H - CO_2 - 2H_2O]^-$ in its ESI-MS/MS spectrum, **M3** was tentatively characterized as shikimic acid [22].

M45 generated $[M - H]^-$ ion at *m/z* 121.028 85 ($C_7H_5O_2$, mass error ≤ ±10.00 ppm). The product ion at *m/z* 93 $[M - H - CO]^-$ appeared in the ESI-MS^2 spectra, which suggested the presence of carbonyl group. Therefore, **M45** was tentatively characterized as benzoic acid.

M44 yielded the deprotonated molecule ion at *m/z* 179.070 27 ($C_{10}H_{11}O_3$, mass error ≤ ±10.00 ppm). Furthermore, it gave rise to the characteristic product ion at *m/z* 135 $[M - H - CO_2]^-$, which indicated the presence of carbonyl group in its molecular. Therefore, **M44** was tentatively characterized as methyl 2-ethoxybenzoate.

M22 possessed the theoretical $[M - H]^-$ ion at *m/z* 137.023 32 ($C_7H_5O_3$, mass error ≤ ±10.00 ppm). It was 16 Da more than that of benzoic acid, indicating that it might be hydroxylation product of benzoic acid. Meanwhile, combined with the product ions at *m/z* 93 $[M - H - CO_2]^-$ and *m/z* 109 $[M - H - H_2O]^-$, **M22** was tentatively characterized as 3-hydroxybenzoic acid.

M11 afforded the deprotonated molecule ion at *m/z* 153.018 23 ($C_7H_5O_4$, mass error ≤ ±10.00 ppm). It yielded the product ion at *m/z* 109 $[M - H - CO_2]^-$, suggesting the presence of the carboxyl group in its molecule. Therefore, **M11** was characterized as 3,4-dihydroxybenzoic acid.

M14 and **M34** generated the same $[M - H]^-$ ions at *m/z* 178.049 86 ($C_9H_8NO_3$) with mass error within ±10.00 ppm. In addition, DPI at *m/z* 134 $[M - H - CO_2]^-$ indicating the occurrence of a carboxyl group was also observed. Therefore, **M14** and **M34** were characterized as hippuric acid or its isomer.

M23 yielded $[M - H]^-$ ion at *m/z* 194.044 78 ($C_8H_8NO_4$) with mass error within ±10.00 ppm. Additionally, it was 16 Da more than that of hippuric acid. Moreover, DPI at *m/z* 135 $[M - H - CO_2 - CH_3]^-$ and product ion at *m/z* 150 $[M - H - CO_2]^-$ indicating the occurrence of carboxyl group and methyl group were observed. Therefore, **M23** was tentatively characterized as 3-hydroxyl hippuric acid.

M1, **M10** and **M62** afforded the deprotonated molecule ion at *m/z* 197.044 45 ($C_9H_9O_5$, mass error ≤ ±10.00 ppm). Then the ion at *m/z* 197 further yielded a series of characteristic product ions at *m/z* 167, *m/z* 149 and *m/z* 121. According to the previously reported literature, **M1**, **M10** and **M62** were tentatively characterized as syringic acid or its isomers [27].

In the ESI-MS^2 spectra of **M5**, **M7**, **M8** and **M13**, the $[M - H]^-$ ions at *m/z* 167.033 88 ($C_8H_7O_4$, error ≤ ±10.00 ppm) generated the fragment ions at *m/z* 123 $[M - H - CO_2]^-$ and *m/z* 149 $[M - H - H_2O]^-$, indicating the presence of carboxyl and hydroxyl groups. Therefore, they were tentatively characterized as vanillic acid or its isomers.

M17, **M47** and **M67** afforded $[M - H]^-$ ions at *m/z* 355.102 35 ($C_{16}H_{19}O_9$, mass error ≤ ±10.00 ppm) with the retention time ranging from 6.91 to 11.04 min. They were 2 Da more than that of prototype drug, indicating that they may be the hydrogenation products of CQA. Meanwhile, the characteristic product ion at *m/z* 191.0561 $[M - H - C_9H_8O_3]^-$ (quinic acid skeleton) and *m/z* 173.0455 $[M - H - C_9H_{10}O_4]^-$ in their ESI-MS^2 spectra suggested the presence of quinic acid group. Then it yielded the fragment ion at *m/z* 181.0495 $[M - H - C_7H_{10}O_5]^-$ (dihydro-caffeic acid skeleton), which indicated the existence of dihydro-caffeic acid group. The fragment ion at *m/z* 137.0233 were also observed, which were formed by neutral loss of 44 Da (CO_2) from the ion at *m/z* 181.0495. Therefore, they were tentatively characterized as dihydro-CQA isomers [28].

M38, **M49**, **M58** and **M63** were extracted in the HREIC at *m/z* 367.104 00 ($C_{17}H_{19}O_9$, mass error ≤ ±2.00 ppm) with retention time from 8.92 to 10.42 min. They all possessed the similar DPIs at 179.0350 (caffeic acid skeleton) and *m/z* 135.0452. Besides, the DPIs *m/z* 191.0561 ([quinic acid – H]$^-$) and *m/z* 173.0455 ([quinic acid – H_2O – H]$^-$) also existed. And thus, they tended to be methylation products of CQA [28].

M41, **M52**, **M55**, **M57**, **M59** and **M61** showed the same $[M - H]^-$ ions at *m/z* 369.11801 ($C_{17}H_{21}O_9$, mass error within ±10.00 ppm). They were 2 Da more than that of methyla-

tion product of CQA. In their ESI-MS^2 spectra, there were abundant product ions at *m/z* 191 [quinic acid – H]$^-$, *m/z* 173 [quinic acid – H – H_2O]$^-$ and product ions at *m/z* 181 [dihydrocaffeic acid – H]$^-$ and *m/z* 137 [dihydrocaffeic aciddihydrocaffeic acidCO_2 – H]$^-$, indicating that they were hydrogenation and methylation products of CQA.

M72 eluted at 13.82 min yielded [M – H]$^-$ ion at *m/z* 543.170 83 ($C_{24}H_{31}O_{14}$). It was 176 Da more than that of methyl CQA, suggesting the presence of glucuronidation group in the molecule. Therefore, in combination with the DPIs at *m/z* 173 [quinic acid – H_2O – H]$^-$, *m/z* 135 [caffeic acid – CO_2 – H]$^-$ and product ion at *m/z* 367 [M – H – glucose]$^-$, **M72** was characterized as glucose conjugation product of methyl CQA.

Both **M15** and **M24** afforded [M – H]$^-$ ions at *m/z* 433.043 52 ($C_{16}H_{17}O_{12}S$, mass error ≤ ±10.00 ppm). They further yielded a series of DPIs (*m/z* 191 [quinic acid – H]$^-$, *m/z* 173 [quinic acid – H_2O – H]$^-$ and *m/z* 135 [caffeic acid – CO_2 – H]$^-$) and product ion (*m/z* 353 [M – H – SO_3]$^-$). The fact that they were 80 Da more than that of prototype drugs, suggested the presence of sulfonation group in their molecules. Therefore, they were tentatively characterized as sulfate conjugation products of CQA.

M26, **M31** and **M46** afforded the deprotonated molecule ion at *m/z* 529.1199 ($C_{23}H_{29}O_{14}$, mass error ≤ ±1.00 ppm). They were 176 Da more than that of the prototype drug, suggesting the presence of a glucuronide group in their molecules. Furthermore, in combination with the observed DPIs (*m/z* 353 [M – H – 176]$^-$, *m/z* 191 [quinic acid – H]$^-$, *m/z* 173 [quinic acid – H_2O – H]$^-$ and *m/z* 135 [caffeic acid – H – CO_2]$^-$), they were tentatively characterized as glucuronide conjugation products of CQA.

M6 generated the deprotonated molecule ion at *m/z* 435.059 17 ($C_{16}H_{20}O_{12}S$, mass error ≤ ±10.00 ppm). It was 80 Da more than that of dihydro-CQA, indicating that the sulfation reaction probably occurred. Moreover, the product ions at *m/z* 417 [M – H – H_2O]$^-$, *m/z* 181 [Dihydrocaffeic acid – H]$^-$ and *m/z* 261 [Dihydrocaffeic acid – H + SO_3]$^-$) were also observed. Therefore, **M6** was tentatively characterized as sulfate conjugation product of dihydro-CQA.

Comparative metabolism study on 5-CQA, 4-CQA and 3-CQA in rats

In this study, all the *in vivo* metabolites of 5-CQA, 4-CQA and 3-CQA in rat plasma, urine and faeces were compared comprehensively (Figs. 3, S3, and 4). Summarizing the metabolic pathways of 73 metabolites identified in rats respectively administrated with 5-CQA, 4-CQA and 3-CQA, three main biotransformation pathways producing metabolites were listed as follows: Firstly, positional isomerism was prone to engender during biotransformation. For instance, the caffeoyl on quinic acid was easy to migrate, which resulted in the mutual transformation among 5-CQA, 4-CQA and 3-CQA. Secondly, 5-CQA, 4-CQA and 3-CQA could be easily hydrolyzed into caffeic acid and quinic acid, which were immediately followed by a series of metabolic reactions including sulfate conjugation, methylation and sulfate conjugation, acetylation and glucuronide conjugation. In addition, some biotransformation pathways were also observed based on the prototype drugs, such as methylation, hydrogenation, and so on.

Individually, there were many specific metabolites generated for these three CQAs. For example, a total of 16 metabolites were found solely for 5-CQA mostly involved in sulfate conjugation, methylation, cysteine glycine conjugation, *etc*. Meanwhile, 10 metabolites were only detected in the metabolic profiling of 4-CQA, including hydrogenation, methylation, and so on. In contrast, relatively few special metabolites were screened and identified for 3-CQA.

Moreover, during the biotransformation process, prototype drugs usually yielded the intermediate metabolites at first, and then the further metabolic reactions occurred based on these intermediate metabolites. Therefore, the intermediate metabolites were usually regarded as main essential ingredients among the metabolic profiling, such as 5-CQA, 4-CQA, 3-CQA, qunic acid, caffeic acid, ferulic acid and isoferulic acid (Fig. 5). The rest metabolites generated from these essential metabolites were often in extremely low quantity. Therefore, when Network Pharmacology was applied to interpret the anti-inflammatory mechanism for those three CQAs, three prototype drugs (5-CQA, 4-CQA, 3-CQA) and four essential metabolites (qunic acid, caffeic acid, ferulic acid and isoferulic acid) were adopted as the research objects.

Network pharmacology for anti-inflammation mechanism study

Target prediction acting on inflammation and compounds

In total, 36 115 known targets for inflammation were collected from database [29]. The details were described in Table S2. Furthermore, the number of putative targets for 7 essential metabolites was summed up to 649 by eliminating the overlapping values. Detailed information about putative targets is provided in Table S3. As a result, a total of 159 anti-inflammatory potential targets were screened by selecting intersection (Table S4).

Networks and its features

After eliminating the overlapping proteins, a compound-target network was constructed on the basis of 7 metabolites (5-CQA, 4-CQA, 3-CQA, qunic acid, caffeic acid, ferulic acid and isoferulic acid) and their targets. As shown in Fig. 6, the network was composed of 166 nodes and 648 edges. System biology studies had shown that genes and proteins were interconnected and the PPI Networks were relevant to understand the role of various proteins involved in complex diseases (Table S5) [30]. Finally, we obtained the PPI relationship (Fig. 6), which consisted of 159 nodes and 1046 edges. The essential proteins were found to occur in both inflammation associated and compounds target Networks: GAPDH, ALB, TP53, MAPK1, ESR1, HRAS, MAPK8, MAPK14 and SOD1, which played an important role in the response to 7 metabolites in the anti-inflammation activities.

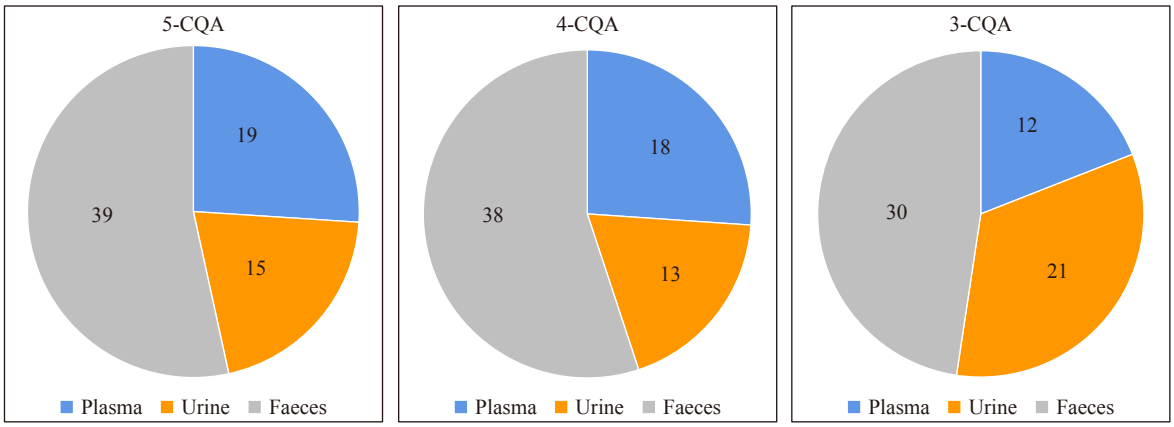

Fig. 3 Distribution for metabolites of 5-CQA, 4-CQA, 3-CQA in rat plasma, urine and faeces

Fig. 4 Veen diagram of the metabolites of 5-CQA, 4-CQA and 3-CQA

And the related parameters (Degree, Betweenness and Closeness) of essential proteins was shown in Table S6.

Enrichment analysis

The biological processes (BP), molecular functions (MF)

and cellular component (CC) of 7 metabolites were analyzed using FunRich software. The results showed that these targets were enriched into 20 biological processes, 51 molecular functions and 92 cell components (Table S7). Meanwhile, 159 interactive targets involved 642 signal pathways in KEGG Enrichment analysis (Table S8). The top ten pathways ($P < 0.01$) were p75 (NTR)-mediated signaling, MAPK related pathways, Glutathione conjugation, S1P2 pathway, TNF receptor signaling pathway, p38 MAPK signaling pathway, ALK1 pathway, Phase II conjugation, Biological oxidations and dopamine degradation (Figs. 6C and 6D). Based on these data, we speculated that components could exert anti-inflammatory effects by mediating the related pathways involved in hormone levels, DNA transcription, receptor expression and metabolism, and so on.

Conclusions

Due to the low absorption efficiency of 5-CQA, 4-CQA and 3-CQA, it is difficult to reveal their metabolic behavior of three compounds [31-33]. Unless they are administered at a higher dose than clinic dose, their metabolic laws and pathways could be figured out, and thus numerous metabolites were able to be found in different biological samples. Therefore, the larger doses were a necessary prerequisite for studying the compounds' metabolic pathway. Here, we set a dose of 250 mg/kg body weight, which was 10–25 times of the clinic dose. Besides, metabolites identification relied on UHPLC-HRMS, and its advantages to ensure the detection sensitivity. We previously summarized that CQAs could be converted to caffeic acid and quinic acid *in vivo*. This process was accompolished under the action of intestinal flora esterase, which mainly occured in the cecum and colon [34-35]. In this study, 5-CQA, 4-CQA and 3-CQA generated a wide range of metabolites when individually administrated to rats. Moreover, 5-CQA, 4-CQA and 3-CQA mainly underwent similar metabolic pathways including methylation, hydrogenation, glucuronic acid conjugation, sulfonation, isomerization, and so on.

Network Pharmacology results demonstrated that 5-CQA, 4-CQA, 3-CQA and their metabolites exerted an anti-inflammatory effect through co-owned 52 targets. A number of different targets enriched the same metabolic pathway, indicating that 5-CQA and homologs exerted anti-inflammatory activities through similar metabolic pathways. According to the GO analysis result, 5-CQA and its homologs had the same biological and molecular processes. Besides, Network Pharmacology results demonstrated that the sites of exerting efficacy in the body were also highly similar. Most of CQA homolog targets were found to be receptor, transferase, ligase, signaling molecule, hydrolase, phosphatase, and so on, indicating that CQA homolog and their metabolites could act as signal molecules binding to these targets and regulating the biological functions of related targets.

In this study, we revealed that 5-CQA and its two isomers produced 74 metabolites in rats. Moreover, many of these metabolites have not ever been reported. We also summarized a much more systematic metabolic pathways through analysis of prototype drugs and their metabolites, and four ingredients (caffeic acid, quinic acid, ferulic acid and isoferulic acid) were deduced as the most important metabolites, which produced by a series of reactions. It was generally believed that the metabolic components in biological samples have many better biological activities. Therefore, we regarded 5-CQA, 4-CQA, 3-CQA and four main metabolites as the candidate components, and then predicted their anti-inflammatory mechanism of those seven components through Network Pharmacology. Eventually, much more biological information was obtained because four more metabolic components were considered during the analysis. In conclusion, we established a strategy for the differential expression of isomeric components-metabolite profiles-network targets-biological effects for 5-CQA and its homologs, which would provide a new idea for the other similar studies.

Supplementary Materials

Supplementary materials are available as Supporting Information, and can be requested by sending E-mail to the corresponding author.

References

[1] Neil E, Fiona M, Kevin CF, *et al*. Differential effects of the D- and L-isomers of amphetamine on pharmacological MRI-BOLD contrast in the rat [J]. *Psychopharmacology*, 2007, **193**(1): 11-30.

[2] Bai Y, Zheng YY, Pang WJ, *et al*. Identification and characterization of chlorogenic acids, chlorogenic acid glycosides and flavonoids from *Lonicera henryi* L. (Caprifoliaceae) leaves by LC-MS^n [J]. *Phytochemistry*, 2014, **108**(54): 252-263.

[3] Wang LY, Zheng JQ, Wang Y, *et al*. Comparative study on pharmacological effects of DM-phencynonate hydrochloride and its optical isomers [J]. *Acta Pharmacol Sin*, 2005, **26**(10): 1187-1192.

[4] Vinson JA, Chen X. Determination of total chlorogenic acids in commercial green coffee extracts [J]. *J Med Food*, 2019, **22**(3): 314-320.

[5] Shin HS, Satsu H, Bae M, *et al*. Catechol groups enable reactive oxygen species scavenging-mediated suppression of PKD-NFkappaB-IL-8 signaling pathway by chlorogenic and caffeic acids in human intestinal cells [J]. *Food Chem Nutr*, 2017, **9**(2): 165-176.

[6] Yun N, Kang JW, Lee SM. Protective effects of chlorogenic acid against ischemia/reperfusion injury in rat liver: Molecular evidence of its antioxidant and anti-inflammatory properties [J]. *J Nutr Biochem*, 2012, **23**(10): 1249-1255.

[7] Ong KW, Hsu A, Tan BK. Anti-diabetic and anti-lipidemic effects of chlorogenic acid are mediated by ampk activation [J]. *Biochem Pharmacol*, 2013, **85**(9): 1341-1351.

[8] Rie K, Masaru A, Osamu Y, *et al*. Growth suppression of human cancer cells by polyphenolics from Sweetpotato (*Ipomoea batatas* L.) leaves [J]. *J Agric Food Chem*, 2006, **55**(1): 185-190.

[9] Guo XY, Shen X, Long J, *et al*. Structural identification of the metabolites of ganoderic acid B from *Ganoderma lucidum* in rats based on liquid chromatography coupled with electrospray ionization hybrid ion trap and time-of-flight mass

spectrometry [J]. *Biomed Chromatogr*, 2013, **27**(9): 1177-1187.
[10] Zhang JY, Cai W, Zhou Y, *et al*. Profiling and identification of the metabolites of baicalin and study on their tissue distribution in rats by ultra-high-performance liquid chromatography with linear ion trap-Orbitrap mass spectrometer [J]. *J Chromatogr B*, 2015, **985**(1): 91-102.
[11] Luo H, Chen J, Shi LM, *et al*. DRAR-CPI: a server for identifying drug repositioning potential and adverse drug reactions via the chemical-protein interactome [J]. *Nucleic Acids Res*, 2011, **39**(15): 492-498.
[12] Song XQ, Zhang Y, Dai EQ, *et al*. Prediction of triptolide targets in rheumatoid arthritis using network pharmacology and molecular docking [J]. *Int Immunopharmacol*, 2020, **80**(123): 106179.
[13] You JS, Li CY, Chen W, *et al*. A network pharmacology-based study on Alzheimer disease prevention and treatment of Qiong Yu Gao [J]. *BioData Mining*, 2020, **13**(02): 2-32.
[14] Pan LL, Li ZZ, Wang YF, *et al*. Network pharmacology and metabolomics study on the intervention of traditional Chinese medicine Huanglian Decoction in rats with type 2 diabetes mellitus [J]. *J Ethnopharmacol*, 2020, **258**(10): 112842.
[15] Amberger JS. Searching online mendelian inheritance in man (OMIM): A knowledgebase of human genes and genetic phenotypes [J]. *Curr Protoc Bioinformatics*, 2017, **58**(1): 1-12.
[16] Zhu F, Shi Z, Qin C, *et al*. Therapeutic target database update 2012: a resource for facilitating target-oriented drug discovery [J]. *Nucleic Acids Res*, 2012, **40**(12): 1128-1136.
[17] Szklarczyk D, Gable AL, Lyon D, *et al*. STRING protein-protein association Networks with increased coverage, supporting functional discovery in genome-wide experimental datasets [J]. *Nucleic Acids Res*, 2019, **47**(1): 607-613.
[18] Pinero J, Bravo A, Queralt-Rosinach N, *et al*. DisGeNET: a comprehensive platform integrating information on human disease-associated genes and variants [J]. *Nucleic Acids Res*, 2017, **45**(1): 833-839.
[19] Chen JR, Liu C, Cen JM, *et al*. KEGG-expressed genes and pathways in triple negative breast cancer: Protocol for a systematic review and data mining [J]. *Medicine*, 2020, **99**(18): e19986.
[20] Goodwin BL, Ruthven CR, Sandler M. Gut flora and the origin of some urinary aromatic phenolic compounds [J]. *Biochem Pharmacol*, 1994, **47**(12): 2294-2297.
[21] Kunihiro K, Harumi M. Urinary excretion rate and bioavailability of chlorogenic acid, caffeic acid, *p*-coumaric acid, and ferulic acid in non-fasted rats maintained under physiological conditions [J]. *Heliyon*, 2019, **5**(10): 02708.
[22] Silveira JS, Mertz C, Morel G, *et al*. Alcoholic fermentation as a potential tool for coffee pulp detoxification and reuse: Analysis of phenolic composition and caffeine content by HPLC-DAD-MS/MS [J]. *Food Chem*, 2020, **319**(25): 126600.
[23] Farah A, Monteiro M, Donangelo CM, *et al*. Chlorogenic acids from green coffee extract are highly bioavailable in humans [J]. *J Nutr*, 2008, **138**(12): 2309.
[24] Mortele O, Iturrospe E, Breynaert A, *et al*. Optimization of an *in vitro* gut microbiome biotransformation platform with chlorogenic acid as model compound: From fecal sample to biotransformation product identification [J]. *J Pharm Biomed Anal*, 2019, **175**(09): 112768.
[25] Bel-Rhlid R, Thapa D, Kraehenbuehl K, *et al*. Biotransformation of caffeoyl quinic acids from green coffee extracts by *Lactobacillus johnsonii* NCC 533 [J]. *AMB Express*, 2013, **3**: 28.
[26] Ariizumi S, Naito T, Hoshikawa K, *et al*. Simple LC-MS/MS method using core-shell ODS microparticles for the simultaneous quantitation of edoxaban and its major metabolites in human plasma [J]. *J Chromatogr B*, 2020, **1146**: 122121.
[27] Taha GA, Abdel-Farid IB, Elgebaly HA. Metabolomic profiling and antioxidant, anticancer and antimicrobial activities of *Hyphaene thebaica* [J]. *Processes*, 2020, **8**(3): 266-278.
[28] Naranjo PM, Montoliu I, Aura AM, *et al*. *In vitro* gut metabolism of [U-^{13}C]-quinic acid, the other hydrolysis product of chlorogenic acid [J]. *Mol Nutr Food Res*, 2018, **62**(22): 1800396.
[29] Liang NJ, David D, Kitts. Role of chlorogenic acids in controlling oxidative and inflammatory stress conditions [J]. *Nutrients*, 2016, **8**(1): 16-35.
[30] Pang LJ, Liu JP. Comparative effectiveness of 3 Traditional Chinese Medicine treatment methods for idiopathic pulmonary fibrosis: A systematic review and network meta-analysis protocol [J]. *Medicine*, 2019, **98**(30): 16325.
[31] Kumar G, Paliwal P, Mukherjee S, *et al*. Pharmacokinetics and brain penetration study of chlorogenic acid in rats [J]. *Xenobiotica*, 2019, **49**(3): 339-345.
[32] Lafay S, Morand C, Manach C, *et al*. Absorption and metabolism of caffeic acid and chlorogenic acid in the small intestine of rats [J]. *Br J Nutr*, 2006, **96**(1): 39-46.
[33] Xie C, Zhong DF, Chen XY. Metabolites of injected chlorogenic acid in rats [J]. *Acta Pharm Sin*, 2011, **1**: 88-95.
[34] Baba S, Osakabe N, Natsume M, *et al*. Orally administered rosmarinic acid is present as the conjugated and/or methylated forms in plasma, and is degraded and metabolized to conjugated forms of caffeic acid, ferulic acid and m-coumaric acid [J]. *Life Sci*, 2004, **75**(2): 165-178.
[35] Li J, Qin Y, Yu X, *et al*. *In vitro* simulated digestion and in vivo metabolism of chlorogenic acid dimer from *Gynura procumbens* (Lour) Merr: Enhanced antioxidant activity and different metabolites of blood and urine [J]. *J Food Biochem*, 2019, **43**(06): 12654.

Cite this article as: LI Jie, WANG Shao-Ping, WANG Yu-Qi, SHI Lei, ZHANG Ze-Kun, DONG Fan, LI Hao-Ran, ZHANG Jia-Yu, MAN Yu-Qing. Comparative metabolism study on chlorogenic acid, cryptochlorogenic acid and neochlorogenic acid using UHPLC-Q-TOF MS coupled with network pharmacology [J]. *Chin J Nat Med*, 2021, **19**(3): 212-224.